The Optimal Cosmic Epoch for Precision Cosmology

Abraham Loeb
Astronomy Department, Harvard University, 60 Garden Street, Cambridge, MA 02138, USA
(Dated: April 23, 2012)

The statistical uncertainty in measuring the primordial density perturbations on a given comoving scale is dictated by the number of independent regions of that scale that are accessible to an observer. This number varies with cosmic time and diminishes per Hubble volume in the distant past or future of the standard cosmological model. We show that the best constraints on the initial power spectrum of linear density perturbations are accessible (e.g. through 21-cm intensity mapping) at a redshift $z \sim 10$, and that the ability to constrain the cosmological initial conditions will deteriorate quickly in our cosmic future.

Introduction. The early Universe was characterized by linear density perturbations with a fractional amplitude $|\delta(\mathbf{r})| \ll 1$, thought to have been seeded by quantum fluctuations during cosmic inflation across a vast range of scales spanning more than ~ 26 orders of magnitude [1]. As the Universe evolved, these perturbations were processed by its radiation and matter constituents. Recent surveys restricted to a small fraction of the total observable volume of the Universe allowed observers to read off cosmological parameters from the "Rosetta stone" of these density perturbations to an exquisite precision of a few percent [2–4].

In this paper we consider the fundamental limit to the precision of cosmological surveys as a function of cosmic time. Our analysis provides a global perspective for optimizing future observations, and for assessing the ultimate detectability limits of weak features such as non-Gaussianity from inflation [5]. Existing cosmological data sets are far from optimal. For example, the primary anisotropies of the cosmic microwave background (CMB) [4] sample only a two-dimensional (last scattering) surface which represents a small fraction of the three-dimensional information content of the Universe at the redshift of hydrogen recombination, $z \sim 10^3$. In general, three-dimensional mapping is possible using a spectral line [6], such as the 21-cm line of hydrogen [7].

It is convenient to analyze the density perturbations in Fourier space with $\delta_{\mathbf{k}} = \int d^3r\delta(\mathbf{r})\exp\{i\mathbf{k}\cdot\mathbf{r}\}$, where $k = 2\pi/\lambda$ is the comoving wavenumber. The fractional uncertainty in the power spectrum of primordial density perturbations $P(k) \equiv \langle|\delta_{\mathbf{k}}|^2\rangle$ is given by [8, 9],

$$\frac{\Delta P(\bar{k})}{P(\bar{k})} = \frac{1}{\sqrt{N(\bar{k})}}, \tag{1}$$

where the number of independent samples of Fourier modes with wavenumbers between k and $k+dk$ in a spherical comoving survey volume V is,

$$dN(k) = (2\pi)^{-2}k^2V dk, \tag{2}$$

with $N(\bar{k})$ being the integral of $dN(k)/dk$ over the band of wavenumbers of interest around $\bar{k}$.

The maximum comoving wavelength $\lambda_{\rm max}$ that fits within the Hubble radius is set by the condition (see Figure 1),

$$\lambda_{\rm max}(t) = 2R_{\rm H}, \tag{3}$$

where $R_{\rm H} \equiv c/(aH)$ is the comoving radius of the Hubble surface, $a = (1+z)^{-1}$ is the scale factor corresponding to a redshift z (normalized to unity at the present time), and $H(t) = (\dot{a}/a)$ is the Hubble parameter at a cosmic time t. The corresponding minimum observable wavenumber $k_{\rm min}(t) \equiv 2\pi/\lambda_{\rm max}$ naturally gives $\int_0^{k_{\rm min}} dk[dN(k)/dk] \approx 1$. At $z \lesssim 10^3$, $H \approx H_0\sqrt{\Omega_m a^{-3} + \Omega_\Lambda}$. Throughout the paper, we adopt a present-day Hubble parameter value of $H_0 = 70$ km s^{-1} Mpc^{-1} (or equivalently $h = 0.7$) and density parameters $\Omega_m = 0.3$ in matter and $\Omega_\Lambda = 0.7$ in a cosmological constant [4].

Counting Modes. An observational survey is typically limited to a small fraction of the comoving Hubble volume $V_{\rm max} = \frac{4\pi}{3}R_{\rm H}^3$, which evolves with cosmic time. Figure 2 shows that $V_{\rm max}$ starts small, then grows to a maximum at the end of the matter dominated era, and finally diminishes due to the accelerated cosmic expansion.

For the standard cosmological model in which the matter density is dominated by cold dark matter (LCDM), nonlinear structure develops first on small spatial scales (large k) where it erases memory of the initial conditions. We associate the maximum wavenumber $k_{\rm max}$ for which the initial conditions are still in the linear regime with the minimum radius $R_{\rm NL} = \pi k_{\rm max}^{-1}$ of a spherical top-hat window for which the root-mean-square amplitude of density perturbations is unity at the cosmic time of interest [10],

$$\sigma^2(R_{\rm NL}) \equiv \int_0^\infty \frac{4\pi k^2 dk}{(2\pi)^3}P(k)\left[\frac{3j_1(kR_{\rm NL})}{kR_{\rm NL}}\right]^2 = 1, \tag{4}$$

where $j_1(x) = (\sin x - x\cos x)/x^2$ is the first spherical Bessel function. We adopt a present-day normalization of $\sigma(8h^{-1}) = 0.8$ for the standard LCDM power-spectrum with a spectral index $n_s = 1$ [4].

Before nonlinear baryonic structure begins to form ($z \gtrsim 50$) we associate the corresponding minimum wavelength, $\lambda_{\rm min} = 2\pi/k_{\rm max}$, with the Jeans length for the

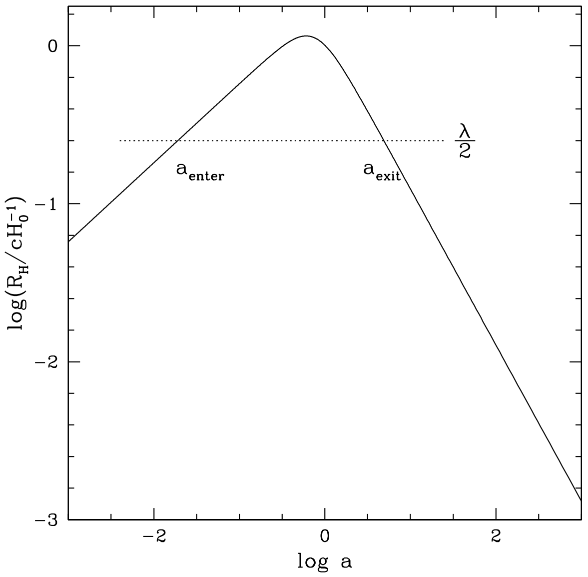

FIG. 1: In the standard (post-inflation) cosmological model, a Fourier mode with a comoving wavelength λ which enters the comoving scale of the Hubble radius $R_{\rm H} = c(aH)^{-1}$ (in units of $cH_0^{-1} = 4.3$ Gpc) at some early time (corresponding to a redshift $z = a_{\rm enter}^{-1} - 1$), would eventually exit the Hubble radius at a later time (corresponding to $a_{\rm exit}$). Hence, there is only a limited period of time when the mode can be observed.

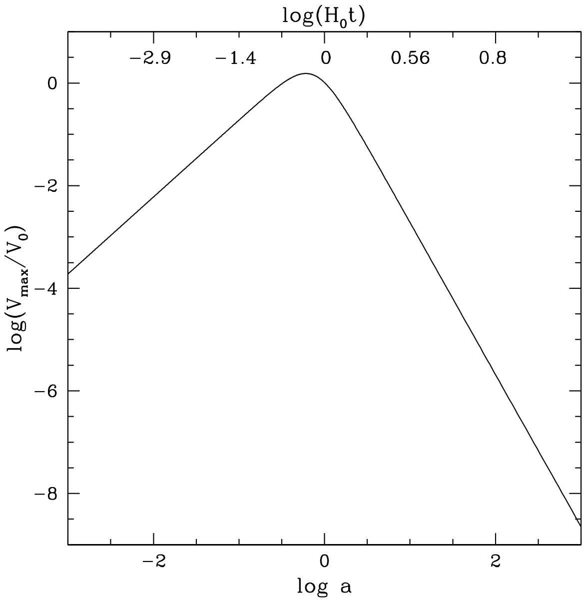

FIG. 2: The Hubble volume $V_{\rm max}$, normalized by its present-day value $V_0 = \frac{4\pi}{3}(c/H_0)^3 = 3.3 \times 10^2$ Gpc^3, as a function of cosmic time t (top axis, in units of the Hubble time $H_0^{-1} = 14$ Gyr) and scale factor $a = (1+z)^{-1}$ (bottom axis).

baryons, $\lambda_{\rm J} = 2\pi/k_{\rm J}$, below which baryonic perturbations are smoothed out by gas pressure. We base this definition on the baryons since they are commonly used by observers to trace the underlying matter distribution. At $z > 200$ when the gas is thermally coupled to the CMB due to the residual fraction of free electrons after cosmological recombination [10],

$$k_J = \left(\frac{2k_B T_{\gamma,0}}{3\mu m_p}\right)^{-1/2} \sqrt{\Omega_m} H_0 = 0.35 \text{ kpc}^{-1}, \qquad (5)$$

where $T_{\gamma,0} = 2.73$K is the present-day CMB temperature, and $\mu = 1.22$ is the mean atomic weight of neutral primordial gas in units of the proton mass m_p. At $z \lesssim 200$ and before the first baryonic objects form, the gas temperature scales as $(1+z)^2$, and so k_J scales up from the value in Eq. (5) as $[(1+z)/200]^{-1/2}$. To keep our discussion simple, we ignore subtleties associated with the motion of the baryons relative to the dark matter [11], the baryonic temperature fluctuations [12], and the X-ray and photo-ionization heating of intergalactic baryons by the first sources of light [13]. These details (which are partially sensitive to the unknown properties of the first sources of light [10]) could reduce $k_{\rm max}$ at $z \gtrsim 10$. Hence, our calculated $k_{\rm max}$ should be regarded as the absolute upper limit, adequate for regions that are not influenced by these effects.

Figure 3 shows the range of wavenumbers between $k_{\rm min}$ and $k_{\rm max}$ that are accessible within the Hubble radius as a function of cosmic time t and scale factor $a(t)$.

The maximum number of linear modes available to an observer at a cosmic time t is then given by,

$$N_{\rm max}(t) = \frac{V_{\rm max}}{12\pi^2}\left(k_{\rm max}^3 - k_{\rm min}^3\right). \qquad (6)$$

The solid line of Figure 4 shows the resulting minimum fractional error in the power-spectrum amplitude $\Delta P(k_{\rm max})/P(k_{\rm max}) = 1/\sqrt{N_{\rm max}}$, as a function of cosmic time and scale factor. We have calculated $R_{\rm NL}$ from equation (4) using the LCDM power spectrum $P(k)$ [4]. The sharp rise in the minimum error at $a \gtrsim 0.1$ occurs because the nonlinear scale $R_{\rm NL}$ increases rapidly above the Jeans length $\lambda_{\rm J}$ around a redshift of $z \sim 10$. The rise is sharp since the root-mean-square amplitude of density fluctuations in LCDM $\sigma(R)$ has a weak R-dependence on small scales, implying that different mass scales collapse at about the same cosmic time. Changing the definition of $R_{\rm NL}$ in Eq. (4) to refer to 2–σ perturbations reaching an overdensity of unity [i.e., $2\sigma(R_{\rm NL}) = 1$] would simply shift this sharp rise to a value of a that is smaller by a factor of 2, since the linear growth factor of perturbations at $z \gg 1$ scales as a.

A present-day observer located at a fixed vantage point can see multiple Hubble volumes of an earlier cosmic time t, which were causally disconnected from each other at that time. The total number of such regions available within a spherical shell of comoving width $\Delta r = 2R_H(t)$

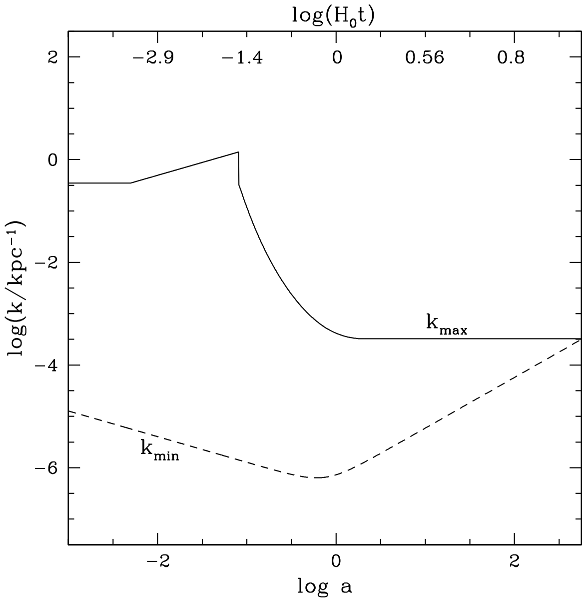

FIG. 3: The range of comoving wavenumbers for which the linear power spectrum can be observed per Hubble volume as a function of cosmic time and scale factor. The minimum wavelength $\lambda_{\min} = 2\pi/k_{\max}$ is taken as the larger among the baryonic Jeans scale and the scale where nonlinear structure forms at any given redshift. The maximum wavelength $\lambda_{\max} = 2\pi/k_{\min}$ is set by the Hubble diameter $2R_{\rm H}$.

is $N_{\rm regions} = (4\pi r^2 \Delta r)/V_{\max}$, where

$$r(t) = \int_t^{t_0} \frac{cdt'}{a(t')}, \tag{7}$$

is the comoving distance to the shell center for observations conducted at the present time t_0. The reduced statistical uncertainty of $1/\sqrt{(N_{\rm regions} \times N_{\max})}$ is shown by the dashed line in Figure 4. Under the most favorable conditions, the probability distribution of density perturbations can be compared to a Gaussian form, $p(\delta)d\delta = (2\pi\sigma^2)^{-1/2} \exp\{-\delta^2/2\sigma^2\}d\delta$, to within a precision of $\sim 10^{-9}$, several orders of magnitude better than the level required for detecting non-Gaussianity from inflation [5]. Measurements of the gravitational growth of $P(k)$ for a particular k at multiple redshifts could test for modifications of general relativity or hidden constituents of the Universe to a similar level of precision.

Conventional observational techniques, such as galaxy redshift surveys, Lyman-α forest spectra, or 21-cm intensity mapping [7, 8, 14], are currently limited by systematic uncertainties (involving instrumental sensitivity and contaminating foregrounds) to levels that are well above the ultimate precision floor presented in Figure 4. But as advances in technology will break new ground for more precise measurements [15], they might offer a qualitatively new benefit – enabling observers to witness the evolution of cosmological quantities [such as $P(k,z)$] in real time over timescales of years [16, 17].

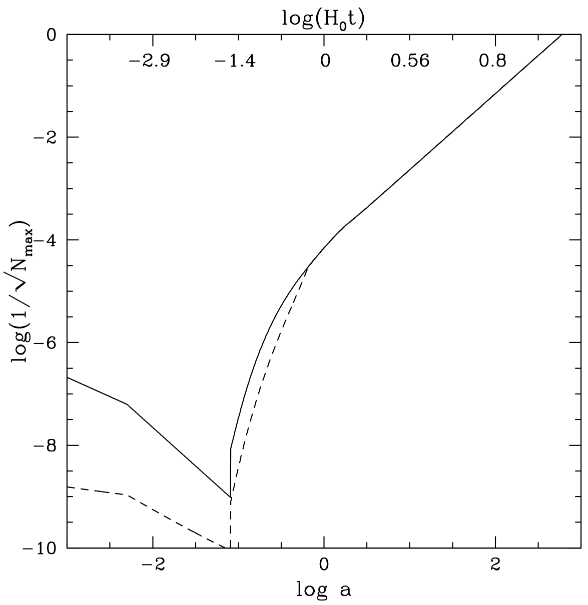

FIG. 4: The minimum fractional error attainable for the power-spectrum amplitude $1/\sqrt{N_{\max}}$ per Hubble volume, as a function of cosmic time and scale factor (solid line). The dashed line includes the reduction in the statistical uncertainty for a present-day observer who surveys a spherical shell of comoving width $2R_H(t)$ centered at the corresponding cosmic times.

Conclusions. Figure 4 implies that the most accurate statistical constraints on the primordial density perturbations are accessible at $z \sim 10$, when the age of the Universe was a few percent of its current value (i.e., hundreds of Myr after the Big Bang). The best tool for tracing the matter distribution at this epoch involves intensity mapping of the 21-cm line of atomic hydrogen [7, 8, 14]. Although the present time ($a = 1$) is still adequate for retrieving cosmological information with subpercent precision, the prospects for precision cosmology will deteriorate considerably within a few Hubble times into the future. For simplicity, our quantitative results were derived for a Universe with a true cosmological constant. However, the ultimate loss of information holds for any type of accelerated expansion, even if the dark energy density is evolving in time.

For pedagogical purposes, we considered the instantaneous number of modes available on a space-like hypersurface of a fixed cosmic time t, under the assumption that a typical cosmological survey would focus on a small fraction of $V_{\max}(t)$ in which the constant time approximation is valid. Otherwise, the evolution of the density field and its tracers needs to be taken into account.

Since the past lightcone of any observer covers volumes of the Universe at earlier cosmic times, one might naively assume that the accessible information only increases for late-time observers, as past information will stay recorded near the horizon even in the distant future [20, 24, 25]. However, in practice the exponential expansion will erase all this information in the future [18–23]. Beyond a hundred Hubble times (a trillion years from now), the wavelength of the CMB and other extragalactic photons will be stretched by a factor of $\gtrsim 10^{29}$ and exceed the scale of the horizon [26] (with each photon asymptoting towards uniform electric and magnetic fields across the Hubble radius), making current cosmological sources ultimately unobservable. While the amount of information available now from observations of our cosmological past at $z \sim 10$ is limited by systematic uncertainties that could potentially be circumvented through technological advances, the loss of information in our future is unavoidable as long as cosmic acceleration will persist.

Acknowledgments. I thank Charlie Conroy and Adrian Liu for comments on the manuscript. This work was supported in part by NSF grant AST-0907890 and NASA grants NNX08AL43G and NNA09DB30A.

[1] D. H. Lyth, & A. R. Liddle, The Primordial Density Perturbation: Cosmology, Inflation and the Origin of Structure, Cambridge University Press (2009).
[2] K. T. Mehta, et al., Mon., Not. R. Astron. Soc., submitted (2012); [arXiv:1202.0092]
[3] R. Keisler, et al., Astrophys. J. **743**, 28 (2011).
[4] E. Komatsu, et al., Astrophys. J. Supp. **192**, 18 (2011).
[5] J. M. Maldacena, J. High Energy Phys. **5**, 13 (2003).
[6] C. J. Hogan, & M. J. Rees, Mon. Not. R. Astron. Soc. **188**, 791 (1979); A. Loeb, Astrophys. J. **555**, L1 (2001).
[7] J. Pritchard, & A. Loeb, Rep. Prg. Phys., in press (2012); [arXiv:1109.6012].
[8] A. Loeb, & J. S. B. Wyithe, Phys. Rev. Lett. **100**, 1301 (2008).
[9] Y. Mao, et al., Phys. Rev. **D78**, 3529 (2008).
[10] A. Loeb, & S. Furlanetto, "The First Galaxies in the Universe", Princeton University Press, in press (2012).
[11] D. Tseliakhovich, & C. M. Hirata, Phys. Rev. **D82**, 3520 (2010); D. Tseliakhovich, R. Barkana, & C. M. Hirata, Mon. Not. R. Astron. Soc. **418**, 906 (2011); A. Stacy, V. Bromm, & A. Loeb, Astrophys. J. Lett. **730**, L1 (2011). Note that $\lambda_{\rm min}$ is proportional to the speed of the baryons relative to the dark matter, whose root-mean-square value is larger than the gas sound speed by a factor of ~ 2 in the redshift range $z = 10$–100, increasing $\log(N_{\rm max}^{-1/2})$ in Figure 4 by a modest increment of ~ 0.5 dex. For a Gaussian velocity field, there are special regions where the change is even smaller.
[12] S. Naoz, N. Yoshida, & R. Barkana, Mon. Not. R. Astron. Soc. **416**, 232 (2011).
[13] J. Pritchard, & A. Loeb, Phys. Rev. **D78**, 3511 (2008); *ibid* **D82**, 3006 (2010).
[14] A. Loeb, & M. Zaldarriaga, Phys. Rev. Lett. **92**, 1301 (2004).
[15] S. Lopez, Science **321**, 1301 (2008).
[16] A. Sandage, Astrophys. J. **136**, 319 (1962).
[17] A. Loeb, Astrophys. J. **499**, L111 (1998).
[18] T. Rothman, & G. F. R. Ellis, The Observatory **107**, 24 (1987).
[19] A. A. Starobinsky, Grav. Cosm. **6**, 157 (2000);
[20] A. Loeb, Phys. Rev. **D65**, 047301 (2002). See also §8 in A. Loeb, "How Did the First Stars and Galaxies Form?", Princeton Univ. Press (2010).
[21] T. Chiueh, & X.-G. He, Phys. Rev. **D65**, 123518 (2002).
[22] E. H. Gudmundsson, & G. Björnsson, Astrophys. J. **565**, 1 (2002).
[23] L. M. Krauss, & R. J. Scherrer, General Relativity and Gravitation **39**, 1545 (2007); see also L. M. Krauss, & G. D. Starkman, Astrophys. J. **531**, 22 (2000).
[24] K. Nagamine, & A. Loeb, New Astronomy **8**, 439 (2003); *ibid* **9**, 573 (2004). See also, Y. Hoffman, et al., JCAP **10**, 16 (2007); P. Araya-Melo, et al., Mon. Not. R. Astron. Soc. **399**, 97 (2009).
[25] M. T. Busha, et al., Mon Not R. Astron. Soc. **363**, L11 (2005); see also Astrophys. J. **596**, 713 (2003) and Astrophys. J. **665**, 1 (2007).
[26] A. Loeb, JCAP **4**, 23 (2011).